Quantum Electronics **49** (7) 693–697 (2019)

OPTICAL FIBRES

https://doi.org/10.1070/QEL16833

Erbium-doped optical fibre with enhanced radiation resistance for superluminescent fibre sources

A.A. Ponosova, I.S. Azanova, N.K. Mironov, M.V. Yashkov, K.E. Riumkin, O.L. Kel', Yu.O. Sharonova, M.A. Melkumov

Abstract. **This paper presents a study of the properties of erbium-doped optical fibres with enhanced gamma-ray resistance at a high dose rate. The fibres have a silica core containing different dopants. The gamma-ray resistance of the fibres is due to additional doping of their core with cerium and germanium ions, as well as to aluminium concentration optimisation. We assess the effect of fibre composition on the radiation-induced loss at a wavelength of 1310 nm and the output power and weighted average wavelength of superluminescent fibre sources based on erbium-doped fibre under pulsed gamma irradiation (dose per pulse, ~20 Gy). The fibre doped with aluminium, germanium and cerium oxides is shown to be optimal for use in gamma-ray-resistant broadband superluminescent fibre sources.**

Keywords: *superluminescent fibre source, optical fibre, erbium, cerium, ionising radiation, gamma rays, radiation resistance, radiation-induced loss.*

1. Introduction

Superluminescent fibre sources (SFS's) based on erbium-doped optical fibre are preferred light sources for interferometric fibre-optic sensors, especially for navigational-accuracy fibre-optic gyros (FOGs) [1]. In a number of important applications, SFS's can be exposed to gamma rays [2, 3]. Interaction of gamma photons with optical materials leads to the formation of radiation-induced colour centres, which absorb light in both the visible and IR spectral regions [4, 5]. This can cause a considerable decrease (by more than a hundred times) in the output power of the SFS [6].

In most cases, SFS's should be resistant to prolonged continuous exposure (for years or tens of years) to ionising radiation at a relatively low dose rate, so that in the case of, e. g., typical space missions the total dose is at a level of a few kilograys. Issues pertaining to the performance stability of SFS's under continuous gamma irradiation have been the subject of extensive studies (see Refs [6–13] and references therein). At the same time, some conventional [14] and a number of special applications [15–17] require that fibre withstand exposure to pulsed radiation at a comparatively high dose rate. Short-term exposure to ionising radiation with an appreciable gamma-ray dose occurs e. g. during lightning discharges (frequent phenomena, accompanied by low-intensity ionising radiation surges) [18], solar flares (with a frequency from several times per year in the case of low flare intensities to once in several tens of years at intermediate flare intensities), supernova explosions in our Galaxy (one or two events per year, with an intermediate ionising radiation intensity) and explosions of higher power systems (neutron stars, black holes and others, with a comparatively high intensity). The exposure to ionising radiation during such events lasts milliseconds to several hours. The accumulated radiation dose can range from a fraction of a milligray to hundreds and even thousands of grays (in the case of very seldom events), depending on the proximity and scale of the event. In this work, we restricted ourselves to relatively frequent events that do not lead to any catastrophic consequences on the Earth, in which the total dose does not exceed a few or tens of grays. For this reason, we chose a dose at a level of 20 Gy for pulsed exposure. The exposure time was determined not so much by the characteristic times of the possible events under consideration as by the time performance of available equipment for such studies (tens of nanoseconds).

The objectives of this work were to optimise the core composition of erbium-doped fibre so as to ensure high (or enhanced) radiation resistance in combination with a broad luminescence band, and to understand general trends of variations in the output power and emission spectra of SFS's exposed to ionising radiation.

2. Measurement technique and experimental data obtained without irradiation

2.1. Fabrication and properties of erbium-doped fibres

Erbium-doped fibres with different compositions were designed and fabricated at the Fiber Optics Research Center,

A.A. Ponosova JSC Perm Scientific Industrial Instrument Making Company, ul. 25 Oktyabrya 106, 614007 Perm, Russia; A.M. Prokhorov General Physics Institute, Russian Academy of Sciences, ul. Vavilova 38, 119991 Moscow, Russia; e-mail: nastya-aleksi@mail.ru;
I.S. Azanova JSC Perm Scientific Industrial Instrument Making Company, ul. 25 Oktyabrya 106, 614007 Perm, Russia; Perm State University, ul. Bukireva 15, 614990 Perm, Russia; e-mail: azanova@ppk.perm.ru;
N.K. Mironov Russian Federal Nuclear Center 'All-Russian Research Institute of Experimental Physics', prosp. Mira 37, 607188 Sarov, Nizhny Novgorod region, Russia; e-mail: mironovn@expd.vniief.ru;
M.V. Yashkov G.G. Devyatykh Institute of Chemistry of High-Purity Substances, Russian Academy of Sciences, ul. Tropinina 49, 603951 Nizhny Novgorod, Russia; e-mail: yashkovmv@yandex.ru;
K.E. Riumkin, M.A. Melkumov Fiber Optics Research Center, Russian Academy of Sciences, ul. Vavilova 38, 119333 Moscow, Russia; e-mail: 3bc@mail.ru, melkoumov@fo.gpi.ru;
O.L. Kel', Yu.O. Sharonova JSC Perm Scientific Industrial Instrument Making Company, ul. 25 Oktyabrya 106, 614007 Perm, Russia; e-mail: kel@ppk.perm.ru, sharonova@pnppk.ru

Received 5 October 2018; revision received 27 March 2019
Kvantovaya Elektronika **49** (7) 693–697 (2019)
Translated by O.M. Tsarev

Russian Academy of Sciences (RAS), in cooperation with researchers from the G.G. Devyatykh Institute of Chemistry of High-Purity Substances, RAS. Fibre preforms were produced by the MCVD process. The fibres differed in core composition (Table 1).

Table 1. Core glass compositions.

Sample	Core composition	Absorption peak of Er^{3+} at λ = 1530 nm (dB m^{-1})	Dopants			
			Ce	P	Al	Ge
A	P_2O_5(Er/Ce)	3.7	+	+		
B	Al_2O_3(Er/Ce)	6 ± 2	+		++	
C1	Al_2O_3–GeO_2(Er/Ce)	20 ± 5	+		++	++
C2	Al_2O_3–GeO_2(Er/Ce)	25 ± 5	+		+	++
C3	Al_2O_3–GeO_2(Er/Ce)	25 ± 5	+		+	+

The core of all samples contained cerium ions, because this variable valency element helps to reduce the concentration of radiation-induced colour centres. Ce (III) and Ce (IV) are known to be highly effective in eliminating hole and electron colour centres [4]. Note that, unlike in the case of other known variable valency ions (for example, iron and nickel), doping with cerium does not increase the optical loss in the IR spectral region. Moreover, the two valency states of cerium can readily be changed by ionising radiation. The cerium concentration in the solution used to impregnate the porous layer of the fibre preforms was roughly the same for all the samples.

The guiding structure of fibre A was formed via doping of the fibre core with phosphorus oxide. The core of sample B was doped with aluminium oxide, and samples C contained aluminium and germanium oxides. The aluminium oxide concentration in the core of sample C1 was approximately a factor of 1.5 higher than that in samples C2 and C3. The germanium oxide concentration in sample C3 was about half that in samples C1 and C2.

Some of the components of the core glass (Si, P, Al and Ge) were deposited from the gas phase onto the inner surface of a silica substrate tube to produce a porous glass layer. Next, the porous layer was impregnated with a solution containing Er^{3+} and Ce^{3+} ions. After solvent removal, it was sintered into a transparent layer. In the final fibre fabrication step, the tubular preform was collapsed into a rod. The preforms were drawn into optical fibre with a second mode cut-off wavelength near 0.95 μm. The optical loss around 1150 nm was within 25 dB km^{-1}.

2.2. Configuration and parameters of superluminescent fibre sources

To study spectral and power characteristics of the erbium-doped fibres exposed to gamma rays, we used a single-pass SFS configuration with a counterpropagating pump beam (Fig. 1). This configuration is suboptimal from the viewpoint of the stability of the weighted average wavelength, spectral width and efficiency, but it allows one to compare the behaviour of different fibres under irradiation, while minimising the influence of other factors (active fibre length, fusion splice loss, reflectivity at the far fibre end and others).

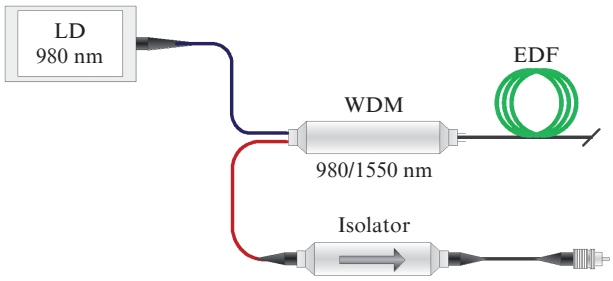

Figure 1. Superluminescent fibre source configuration: (LD) pump laser diode; (WDM) wavelength-division multiplexer; (EDF) erbium-doped fibre.

The erbium-doped fibres were pumped by a semiconductor laser emitting at 980 nm. Pumping at 980 nm makes it possible to reach a higher inversion level in comparison with pumping in the range 1.42–1.48 μm and contributes to active photobleaching of colour centres [19]. The pump laser beam was launched into the active fibre through a 980/1550 nm wavelength-division multiplexer (WDM). To suppress parasitic lasing, a fibre-optic isolator was placed at the output of the device. The active fibre length in the SFS was such that, at a pump power of 150 mW, pump absorption was at least 30 dB.

The emission spectra of the SFS's and their output power as a function of pump power were measured before exposure to ionising radiation. The spectra were obtained in the range 1500–1620 nm with a resolution of 0.1 nm using an optical

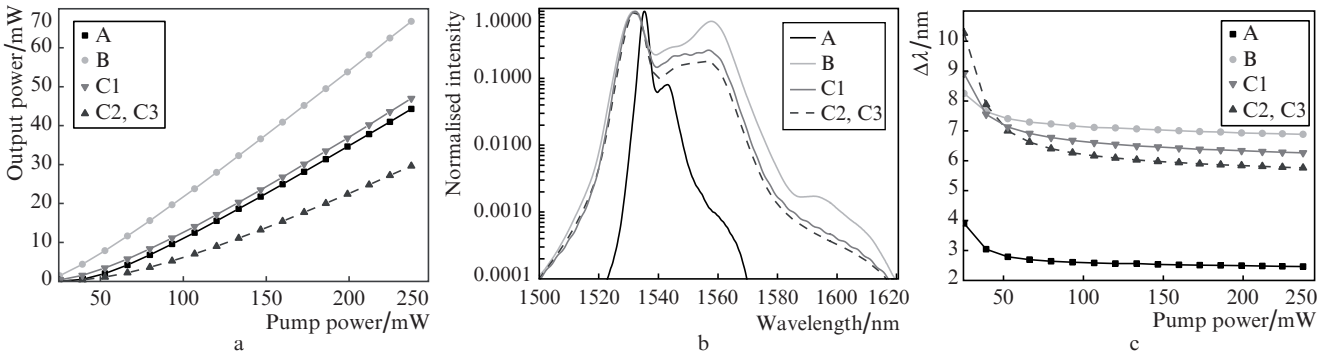

Figure 2. Characteristic output parameters of SFS's with radiation-resistant erbium-doped fibres differing in core composition (samples A, B, C1, C2 and C3): (a) output power as a function of pump power, (b) emission spectra, (c) spectral width $\Delta\lambda$ as a function of pump power (T = 25°C).

spectrum analyser. Figure 2 shows typical spectral and power characteristics of the SFS's based on the erbium-doped fibres under study. The highest slope efficiency, $\eta = 32.5\%$, and the largest full width at half maximum (FWHM) of the SFS output spectrum, $\Delta\lambda = 6.9$ nm, were obtained in the case of the aluminium oxide-doped fibres: Al_2O_3(Er/Ce). The phosphorus oxide-doped fibre, P_2O_5(Er/Ce), had the narrowest emission spectrum: $\Delta\lambda = 2.3$ nm. The spectra of the samples doped with aluminium, cerium and germanium oxides differed little in shape, and the spectral width of the main peak at 1530 nm was about 6.4 nm. Note that the high aluminium concentration in sample C1 compared to samples C2 and C3 led to an increase in the slope efficiency of the SFS by almost a factor of 1.5.

For application in FOGs, preference should be given to SFS's with the largest width and a Gaussian shape of their emission spectrum and the highest output power [20]. According to Wysocki et al. [21], the width of the spectrum of a source for navigational-accuracy FOGs should be at least 5 nm in order to reduce the angular velocity measurement uncertainty due to Rayleigh scattering, cross coupling between different polarisations and the Kerr effect in the sensing fibre loop of FOGs.

Thus, among the single-pass SFS's with a counterpropagating pump beam, the sources with Al_2O_3(Er/Ce)-based fibre are the best suited for use in navigation systems, because P_2O_5(Er/Ce) fibre does not ensure the required spectral width at 1530 nm.

3. Measurement technique and experimental data obtained during exposure to ionising radiation

Resistance to pulsed ionising radiation was studied in the LIU-30 linear induction electron accelerator, which has a continuous bremsstrahlung spectrum [22] and allows one to obtain gamma photons ranging in average energy from 0.8 to 6 MeV [23]. The gamma dose per pulse was about 20 Gy, and the dose rate in our studies was $(3.2-12.5)\times10^8$ Gy s^{-1}.

Only active optical fibre loops were placed in the bremsstrahlung field of the accelerator because such fibre is the most gamma-sensitive component of SFS's [6]. The other optical and electronic components of the experimental schemes were protected from ionising radiation.

We measured the radiation-induced loss (RIL) in the active fibres and monitored variations in the emission spectra and output power of the SFS's during exposure to pulsed gamma rays at temperatures of –60 and +25 °C. The experimental setup is schematised in Fig. 3. The RIL at a wavelength of 1310 nm was measured using erbium-doped fibre segments a factor of 2 shorter than those in SFS's.

The emission spectra of the SFS's were measured continuously in the spectral range 1500–1600 nm during exposure to ionising radiation using an Ocean Optics NIRQuest spectrophotometer. The spectral resolution was ~3 nm, and the time interval between sequential measurements of the spectra was ~15 ms. The weighted average wavelength was determined from the spectra as

$$\lambda_m = \frac{\sum_{i=1}^{n} I_i\lambda_i}{\sum_{i=1}^{n} I_i}, \quad (1)$$

where n is the number of intervals into which the wavelength range of interest was divided and I_i is the power density in the interval with a centre wavelength λ_i.

To assess the change in SFS power and determine the level of RILs at a wavelength of 1.3 μm as a result of exposure to ionising radiation, the output optical power was detected using a photodetector and oscilloscope for about 20 ms before pulsed irradiation and 90 ms after.

The RIL (dB m^{-1}) at a wavelength of 1310 nm was determined as

$$\alpha = \frac{10\log P}{L}, \quad (2)$$

where L (m) is the fibre length and P is the normalised transmitted power (the ratio of the power at the active fibre input before irradiation to that after irradiation).

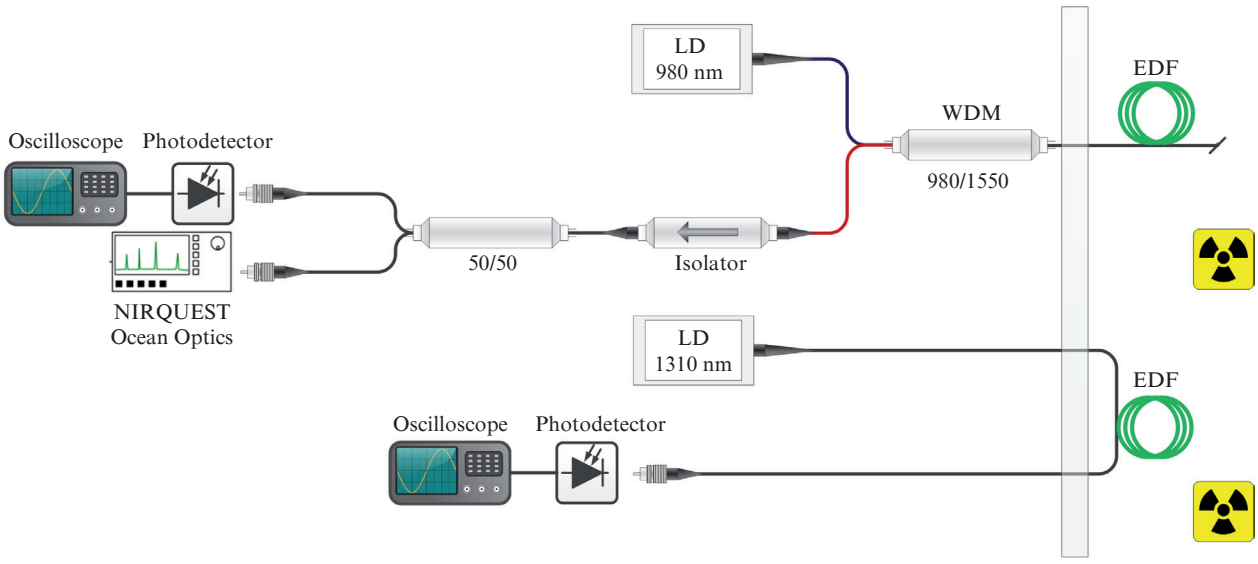

Figure 3. Experimental setups used to study the ionising radiation resistance of the active optical fibres.

4. Results and discussion

Figure 4 illustrates the dynamics of the variation in the power of the SFS's with the active fibres A, B, C1 and C2 in response to a gamma-ray pulse at 25°C. The pulse caused a sharp drop in SFS power, which then rapidly returned to its original level. The output power of sample A, whose core was doped with phosphorus and cerium oxides, returned to its original level in a time less than 1 ms after the end of the pulse. In samples C1 and C2, doped with aluminium, germanium and cerium oxides, the residual SFS power loss after 50 ms was 1% to 2.5%. In sample B, the power loss after 50 ms was above 10%.

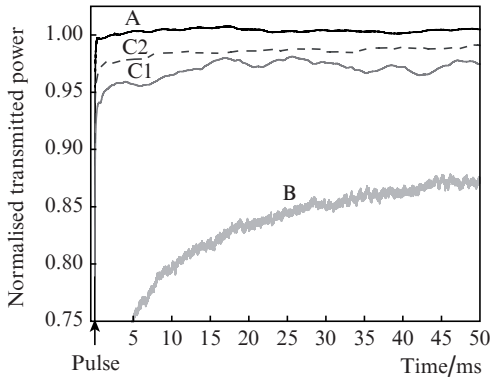

Figure 4. Restoration dynamics of the SFS signal power after exposure of samples A, B, C1 and C2 to a gamma-ray pulse at 25°C.

The low gamma radiation resistance of fibre B is caused by the absence of germanium oxide. In SiO_2–Al_2O_3 and SiO_2–P_2O_5 silica glasses, the RIL is typically due to colour centres related to the formation of nonbridging oxygens at aluminium and phosphorus ions (aluminium–oxygen hole centres and phosphorus–oxygen hole centres). The presence of germanium oxide in glass composition effectively impedes hole centre formation during exposure to ionising radiation [24, 25].

The advantageous effect of germanium oxide on the radiation resistance of the erbium-doped fibres can be demonstrated by comparing their RILs. Figure 5 illustrates the dynamics of the variation in the RIL at a wavelength of 1310 nm in samples A, C1 and C3. The cores of samples C1 and C3 were doped with identical amounts of cerium, but the germa-

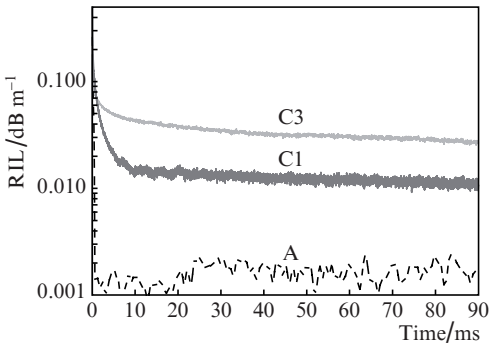

Figure 5. Dynamics of the variation in the radiation-induced loss at a wavelength of 1310 nm after exposure of samples A, C1 and C3 to a gamma-ray pulse at 25°C.

nium oxide concentration in sample C3, which contained less aluminium, was about a factor of 2 lower. The RIL measured after 90 ms in fibre C3, which had a lower GeO_2 concentration, was about three times that in samples C1 and C2.

The highest gamma-ray resistance was offered by sample A. However, as mentioned above, the spectral width of SFS's for application in FOGs should be at least 5 nm. For this reason, optimal fibre samples for SFS's are those containing appreciable amounts of aluminium, which is necessary for reaching the required spectral width at 1530 nm. Moreover, it is seen from the present results that, to reach an enhanced ionising radiation resistance of erbium-doped fibre, the aluminosilicate glass in its core should be additionally doped with considerable concentrations of germanium and cerium oxides.

The effect of ambient temperature on the radiation resistance of erbium-doped fibre was studied at 25 and –60°C using sample C1 as an example. Figure 6 shows time dependences of the output power, weighted average wavelength change ($\delta\lambda_m$) and RIL. It is seen that lowering the temperature has a significant, but not critical, effect on the variation in the parameters of the active fibre under gamma irradiation. The measured RIL at –60°C slightly exceeds that at 25°C. In particular, 100 ms after the end of an ionising radiation pulse the RIL was about 0.006 dB m^{-1} at –60°C and 0.003 dB m^{-1} at 25°C. The output power of the SFS returned in 100 ms to 99% and 97.5% of its original level, respectively. We believe that the lack of a clear correlation between the level of RILs and the drop in SFS power in the test sample is due to two factors:

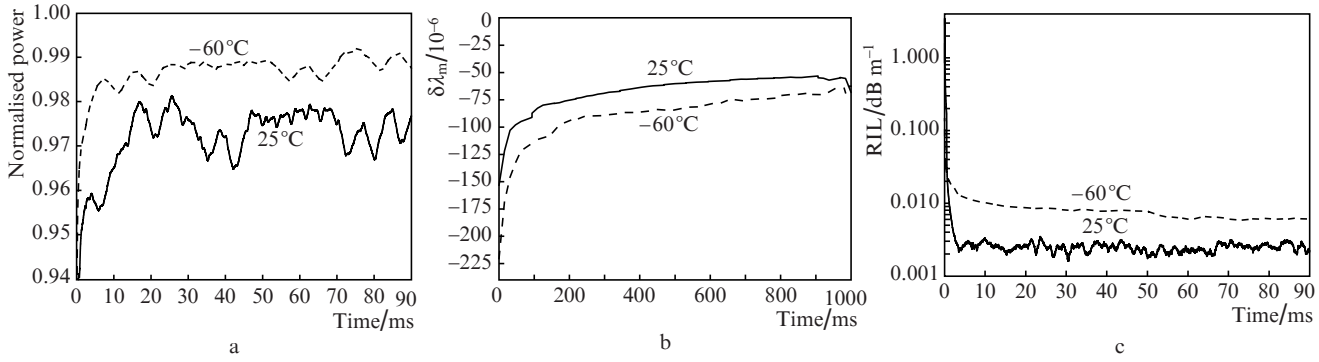

Figure 6. Evolution of the (a) output power, (b) weighted average SFS wavelength and (c) RIL in sample C1 at temperatures of 25 and –60°C.

additional bleaching of the samples under the effect of high pump power and

the difference in the level of RILs at the pump wavelength (980 nm) and test wavelength (1310 nm).

It seems likely that, in the case under consideration, a major contribution to the drop in SFS power is made by the RIL at 980 nm.

At the instant of exposure to ionising radiation, we detected a reduction in weighted average wavelength λ_m. The relative deviation from the value before irradiation was within 1.5×10^{-4} at 25°C and within 2.5×10^{-4} at −60°C. Just 1 s after the irradiation, $\delta\lambda_m$ was within 0.6×10^{-4} at 25°C and within 0.8×10^{-4} at −60°C.

5. Conclusions

The P_2O_5(Er/Ce) fibre has been shown to have the highest resistance to pulsed gamma rays among the samples studied. However, the width of the emission spectrum of SFS's based on such fibre is ∼2.3 nm, which does not meet requirements for the emission spectrum of SFS's for FOGs [21]. The highest slope efficiency, η = 32.5%, and the largest full width at half maximum (FWHM) of the SFS output spectrum, $\Delta\lambda$ = 6.9 nm, have been obtained in the case of the aluminium oxide-doped fibres: Al_2O_3(Er/Ce). Unfortunately, such samples have shown the lowest resistance to pulsed gamma rays.

The optimal fibre for use in gamma-ray-resistant SFS's is the fibre doped with aluminium, germanium and cerium oxides. Optimising the elemental composition of the silica fibre core has made it possible to obtain samples with high radiation resistance and a broad emission spectrum of erbium ions. Exposure of erbium-doped Al_2O_3–GeO_2(Er/Ce) fibre (sample C1) to gamma ray pulses has been shown to sharply reduce the optical power of the SFS: by 10% to 12% at 25°C and by 5% at −60°C. The RIL 0.1 s after the irradiation was 0.006 dB m^{-1} at −60°C and 0.003 dB m^{-1} at 25°C. The largest change in weighted average wavelength was at most 2.5×10^{-4}.

Acknowledgements. We are grateful to A.L. Tomashuk (Fiber Optics Research Center, Russian Academy of Sciences) for helpful discussions and to A.V. Silaev (All-Russia Research Institute of Experimental Physics, Russian Federal Nuclear Center) for his assistance with the measurements at the LIU-30 linear induction electron accelerator.

This work was supported in part by the Perm Scientific Industrial Instrument Making Company and the RF Ministry of Science and Higher Education (Project Nos AAAA-A19-119011690112-0 and AAAA-A19-119012590263-7).

References

1. Aleinik A.S., Kikilich N.E., Kozlov V.N., Vlasov A.A., Nikitenko A.N. *Nauchno-Tekh. Vestn. Inf. Technol., Mekh. Opt.*, **16** (4), 593 (2016).
2. Faussot N., Cottreau Y., Hardy G., Simonpietri P., Gaiffe T. *Proc. SPIE*, **10569**, 105690S (2017).
3. Korkishko Y.N., Fedorov V.A., Prilutskiy V.E., Ponomarev V.G., Morev I.V., Obuhovich D.V., Kostritskii S.M., Zuev A.I., Varnakov V.K., Belashenko A.V., Yakimov E.N., Titov G.V., Ovchinnikov A.V., Abdul'minov I.B., Latyntsev S.V. *Proc. IEEE Intern. Symp. on Inertial Sensors and Systems* (Laguna Beach, CA, USA, 2016) p. 37.
4. Arbuzov V.I. *Osnovy radiatsionnogo opticheskogo materialovedeniya. Uchebnoe posobie* (Introduction to the Irradiation Behaviour of Optical Materials: A Learning Guide) (St. Petersburg: SPb. GUITMO, 2008).
5. Tomashuk A.L., Dvoretskii D.A., Lazarev V.A., Pnev A.B., Karasik V.E., Salganskii M.Yu., Kashaikin P.F., Khopin V.F., Gur'yanov A.N., Dianov E.M. *Vestn. Mosk. Gos. Tekh. Uchilishcha im. N.E. Baumana: Ser. Priborostr.*, **5**, 111 (2016).
6. Li M., Song N., Jin J., Wang X. *Optik (Munich, Ger.)*, **123** (17), 1542 (2012).
7. Girard S., Ouerdane Y., Pinsard E., Laurent A., Ladaci A., Robin T., Cadier B., Mescia L., Boukenter A. *Proc. SPIE*, **10563**, 105632B (2017).
8. Yang Y., Suo X., Yang M. *Proc. SPIE*, 89240W (2013).
9. Peng T.S., Wang L.A., Liu R. *IEEE Photonics Technol. Lett.*, **23** (20), 1460 (2011).
10. Liu C., Zhang L., Wu X., Ruan S. *Opt. Fiber Technol.*, **19** (5), 456 (2013).
11. Yang Y., Suo X., Yang M., Shi X., Jin W. *Proc. SPIE*, **7753**, 775364 (2011).
12. Yuan-Hong Y., Xin-Xin S., Wei Y. *Chin. Phys. B.*, **23** (9), ID 094213 (2014).
13. Jing J. et al. *Chin. Phys. B*, **21** (9), ID 094220 (2012).
14. Tomashuk A.L., Filippov A., Kashaykin P.F., Bychkova E.A., Galanova S.V., Tatsenko O.M., Kuzyakina N.S., Zverev O.V., Salgansky M.Yu., Abramov A.N., Guryanov A.N., Dianov E.M. *J. Lightwave Technol.*, **37** (3), 956 (2019).
15. Greenwell R.A. *Opt. Eng.*, **30** (6), 802 (1991).
16. Tomashuk A.L., Filippov A.V., Moiseenko A.N., Bychkova E.A., Tatsenko O.M., Zavialov N.V., Grunin A.V., Batova E.T., Salgansky M.Yu., Kashaykin P.F., Azanova I.S., Tsibinogina M.K., Levchenko A.E., Guryanov A.N., Dianov E.M. *J. Lightwave Technol.*, **35** (11), 2143 (2017).
17. Girard S., Baggio J., Bisutti J. *IEEE Trans. Nucl. Sci.*, **53** (6), 3750 (2006).
18. Babich L.P., Donskoi E.N., Kutsyk I.M. *Zh. Eksp. Teor. Fiz.*, **134** (1), 65 (2008).
19. Zotov K.V., Likhachev M.E., Tomashuk A.L., Kosolapov A.F., Bubnov M.M., Yashkov M.V., Guryanov A.N., Dianov E.M. *IEEE Photonics Technol. Lett.*, **20** (17), 1476 (2008).
20. Yan Li, Yanfeng Sun, Man Jiang. *Optik (Munich, Ger.)*, **125** (14), 3718 (2014).
21. Wysocki P.F., Digonnet M.J.F., Kim B.Y., Shaw H.J. *J. Lightwave Technol.*, **12** (3), 550 (1994).
22. Pavlovskij A.I., Bossamykin V.S., Gerasimov A.I., et al. *Prib. Tekh. Eksp.*, **41** (2), 13 (1998).
23. Mironov N.K., Gornostai-Pol'skii S.A., Grunin A.V., Zalyalov A.N., Lazarev S.A. *Mezhdunar. nauchn. konf. "XIV Kharitonovskie chteniya"* (XIV Khariton Int. Conf.) (Sarov, 2012) p. 160.
24. Rose T.S., Gunn D., Valley C.G. *J. Lightwave Technol.*, **19** (12), 1918 (2001).
25. Mashinsky V.M., Neustruev V.B., Tomashuk A.L. *Sov. Lightwave Commun.*, **2** (4), 311 (1992).